Sensor systems

A Capacitive Sensor Readout IC With Antenna-Integrated Sensor for Proximity Detection in Handheld Mobile Devices

Ting-Li Hsu[1*], Amelie Hagelauer[1,2**], and Valentyn Solomko[3**]

[1] *Chair of Micro, Nanosystems Technology, Technical University of Munich, 85748 Garching bei München, Germany*
[2] *Fraunhofer EMFT Institute for Electronic Microsystems, Solid State Technologies, 80686 München, Germany*
[3] *Infineon Technologies AG, 85579 Neubiberg, Germany*
[*] *Graduate Student Member, IEEE*
[**] *Senior Member, IEEE*

Manuscript received 29 April 2024; revised 6 June 2024; accepted 12 June 2024. Date of publication 14 June 2024; date of current version 20 June 2024.

Abstract—In this letter, a capacitive sensor readout integrated circuit (IC) and a prototype using an inverted-F antenna (IFA) as the capacitive sensor for proximity detection are presented. A unique front-end circuit converts the single-ended sensing capacitance with one electroplate being always grounded into differential signal utilizing correlated double sampling while suppressing the noise of the front-end circuits. The implemented IC shows that with an offset capacitance of 72 pF, a noise floor of 17 fF can be achieved. The IC was designed and fabricated in a 90 nm RF SOI complementary metal-oxide semiconductor (CMOS) switch technology for its possible integration with radio-frequency (RF) antenna tuning switches. The assembled phone mockup prototype demonstrates the capability of the proposed system to detect the proximity of human body parts with high offset capacitance to maintain the RF performance of the antenna for sub-3GHz mobile communication.

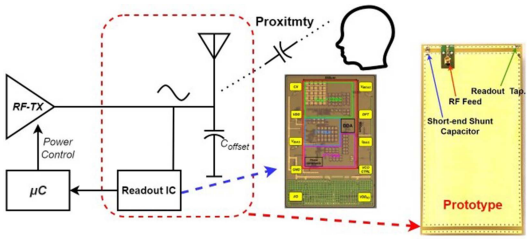

Index Terms—Sensor systems, antenna, capacitive sensor, complementary metal-oxide semiconductor (CMOS), correlated-dobule sampling (CDS), IFA, PIFA, proximity sensor, specific absorption rate (SAR) sensor.

I. INTRODUCTION

Human body parts are exposed to radio-frequency (RF) electromagnetic (EM) fields when using handheld mobile devices, such as a smartphone. In order to minimize the influence of the EM field exposure to health, the specific absorption rate (SAR), a measure of the rate at which the energy is absorbed by unit mass of body tissues, must be limited to 2 W/kg according to the recommendation from International Commission on Nonionizing Radiation Protection [1]. For the purpose of meeting the SAR requirement, transmitted RF power should be reduced if near human body parts are detected. Therefore, a proximity sensor is necessary for modern handheld devices.

Various types of proximity sensors have been brought up based on the detecting mechanism. Optical sensors detect the intensity [2] or the Time-of-Flight [3] of the reflected light to determine the distance between the sensor and near objects. Similar principle can also be applied to ultrasonic proximity sensors [4]. Capacitive–based sensing utilizes the variance of the effective capacitance between sensing electroplates due to the coupling between human body parts and the electroplates [5], [6].

In mobile communication devices, the capacitive sensing is a reasonable option for proximity detection. The use of antennas as sensing electrodes can enable a compact and cost-efficient solution since additional sensor structures are not needed. The feasibility of combining an antenna and a capacitive sensor has been explored in [7]. In [8], a readout circuit based on an *R–C* voltage divider to detect the capacitance between the monopole antenna and the ground plane for proximity sensing is demonstrated. As shown in [8], low offset capacitance value of less than 4 pF can be reached with the monopole antenna, which is a critical factor since the capacitance variation to be detected is around 100 fF. In modern mobile devices, IFA is the most common type of antenna. Conventional IFAs comprise an RF ground at one point along the radiating arm, typically implemented as a dc short. When the IFA is meant to serve as a capacitive sensor read out at low frequencies, the dc short needs to be substituted by an ac short, implemented with a large (as for operating frequency) blocking capacitator, typically in the range of several tens of picofarads. Moreover, the radiating arm of the IFA is a single-ended sensor with one of its electroplate being grounded. As a consequence, the signal-to-noise ratio (SNR) is strongly deteriorated due to the large offset capacitance in parallel to the sensing capacitance. The readout circuit has to be deliberately designed to overcome the negative influence induced by the blocking capacitors.

Antenna systems in modern cellular mobile devices utilize aperture tuning circuits based on solid-state RF switches for improving radiating efficiency over a wide span of frequency bands [9]. A monolithic integration of both antenna tuning and capacitive sensing functions interfacing an in-chassis IFA as a transducer offers a compact and cost-efficient solution for the use in handheld cellular devices.

In this work, a capacitive sensor readout IC designed and fabricated in a 90 nm RF SOI CMOS switch technology is characterized to investigate the feasibility of further integration with antenna tuning switches. A unique front-end has been designed to improve the *SNR of a single-ended one-side-grounded sensor with large offset capacitance*. A phone mockup prototype with its IFA being utilized as capacitive sensor has been assembled to test the readout IC on application level.

Corresponding author: Ting-Li Hsu (e-mail: ting-li.hsu@tum.de).
Associate Editor: Filippo Costa.
Digital Object Identifier 10.1109/LSENS.2024.3414655

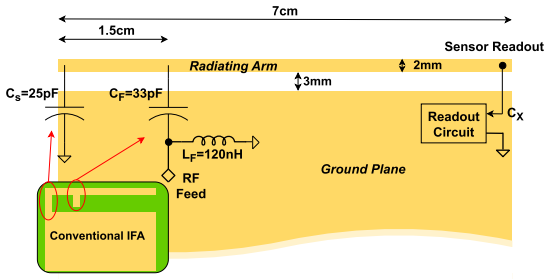

Fig. 1. Proposed IFA as capacitive sensor. The components C_F, C_S, and L_F are actual surface-mounted devices.

II. PROPOSED SENSOR SYSTEM

A. IFA as Capacitive Sensor

IFA is used as the capacitive sensor in this work. Proximity detection is done by sensing the capacitance variation between the radiating arm of the IFA and the ground plane. The design of the IFA-integrated sensor is shown in Fig. 1. The IFA used in this design is modified from the hardware reported in [10] with the detailed dimensions near the radiating element described in Fig. 1. The IFA has been characterized in [9] and [10], demonstrating its suitability for sub-3 GHz cellular bands. The dimension of the radiating arm is designed to cover low cellular bands by having its quarter-wavelength resonant mode at around 730 MHz. The pattern of the radiating arm and the ground plane are on a 1-mm thick FR4 substrate. The dimensions of the total structure are 70 mm × 134 mm to represent the typical size of a modern smartphone. The RF feed is decoupled from the radiating arm by a dc-blocking capacitor C_F with a nominal capacitance of 33 pF, and an RF choke L_F with a nominal inductance of 120 nH shunts the feed port to the ground plane. The short-end of the IFA is dc-decoupled from the ground plane by the capacitor C_S with a nominal capacitance of 25 pF. With the blocking capacitors C_F and C_S, the radiating arm is electrically opened for the low-frequency excitation signal for capacitive sensing while maintaining the RF performance of the IFA. The tapping point for the readout IC is on the open-end of the radiating arm to represent the physical adjacency to the aperture tuner for the future integration.

B. Readout IC

The top-level schematic of the implemented readout IC is shown in Fig. 2. The switches shown in Fig. 2 are controlled by the nonoverlapping clock signals *Ph*1-4 and *AMP*. The signal chain of the readout circuit can be divided into two parts. The first part comprising a low-noise sampling and preamplifying stage converts the capacitance signal from the single-ended sensing capacitor C_X to the differential charge signal stored at C_{SP11} and C_{SP12}. The second part composed of the amplifying and the output stages amplifies the stored differential charge and combines the differential signal into a single-ended output voltage to reduce the number of output pins. Alongside, a built-in switchable testing capacitor bank C_{DFT} with a capacitance value ranging from 0 to 60 fF is placed in parallel to C_X for the characterization of the IC.

The sampling and preamplifying stage is composed of an H-bridge controlled by clock signals *Ph*1-4, balancing capacitors C_{FIX} and C_{DAC}, a charge sense amplifier (CSA) CSA_1 comprised of sampling/resetting switches, C_{AMP1} and OTA_1, and the sample and hold circuit with sampling capacitors C_{SP11} and C_{SP12} following CSA_1. The balancing capacitors C_{FIX} and C_{DAC} are used to prevent CSA_1 from being saturated by the charges from C_X. C_{DAC} is a switchable capacitor bank with a tuning range of up to 20 pF controlled by a 10-bit signal to adapt to the external offset capacitor. Correlated double sampling [11] is utilized to reduce the impact of the noise from OTA_1. Similar approaches have been reported in [12] and [13] for floating sensing capacitors. A novel sampling circuit is designed to adapt the scheme to the single-ended one-side-grounded IFA-integrated sensing capacitor. The principle of the noise-suppressing method is shown in Fig. 3. During *Ph*1, the external sensing capacitor C_X is charged by the supply voltage VDD and the internal balancing capacitors C_{FIX} and C_{DAC} are discharged to ground level. During *Ph*2, the sampling switches of the H-bridge and CSA_1 are switched ON. The voltage on C_X, C_{FIX}, and C_{DAC} is forced to half of VDD through the charge integration process done by OTA_1. As shown in Fig. 3, assuming $C_{DFT} = 0$, the voltage sensed by the capacitor C_{AMP1} in *Ph*2 can be represented as

$$V_{sense1} = \frac{VDD}{2C_{AMP1}} \cdot (C_X - C_{bal}) + \frac{Q_n}{C_{AMP1}} + \frac{Q_{off}}{C_{AMP1}} \tag{1}$$

where

$$C_{bal} = C_{FIX} + C_{DAC} \tag{2}$$

$$Q_n = V_n \cdot (C_{bal} + C_X) \tag{3}$$

$$Q_{off} = V_{off} \cdot (C_{bal} + C_X). \tag{4}$$

V_n and V_{off} are the input referred noise voltage and the offset voltage of OTA_1, respectively. Similar procedure is performed during *Ph*3 and *Ph*4 while C_X is first discharged and C_{bal} is charged to VDD in *Ph*3. The voltage V_{sense2} sensed by C_{AMP1} in *Ph*4 can be written as

$$V_{sense2} = \frac{VDD}{2C_{AMP1}} \cdot (C_{bal} - C_X) + \frac{Q_n}{C_{AMP1}} + \frac{Q_{off}}{C_{AMP1}}. \tag{5}$$

From (3), it is noticeable that the noise in terms of charge/capacitance is larger with larger offset capacitance. For the IFA-integrated sensor in this application scenario, large offset capacitance shunt to the ground plane is inevitable for the RF performance. Hence, CDS is adopted to suppress the low-frequency noise component of V_n. Knowing that $C_{SP11} = C_{SP12}$, the sampled differential charge stored by C_{SP11} and C_{SP12} can be written as

$$Q_{diff} = Q_{C_{SP11}} - Q_{C_{SP12}} = VDD \cdot \frac{C_{SP11}}{C_{AMP1}} \cdot (C_{bal} - C_X) \tag{6}$$

if only the low-frequency component of V_n is taken into consideration. In order to effectively reduce the noise from OTA_1, the sampling frequency is set to 30 kHz while the signal bandwidth of interest is 500 Hz. During *Ph*2 and *Ph*4, a total capacitance $C_{tot} = C_{bal} + C_X$ is charged or discharged to half of VDD through OTA_1. Each phase lasts for 5.7 μs. In order to reduce the sampling error from the charging and discharging process, the transconductance of OTA_1 is designed to be 400 μS, which results in an R–C time constant of 0.375 μs with $C_{tot} = 150$ pF. With higher transconductance, the noise from OTA_1 can also be further reduced since the broadband white noise is not removable with CDS.

In the amplifying and output stage, the differential charge Q_{diff} is sensed and amplified by CSA_2 during the phase AMP. The amplified signal is held by C_{SP21} and C_{SP22} and converted to a single-ended signal with a differential difference amplifier (DDA) DDA_1 [14]. With the output voltage V_{MEAS} fed back to the negative input of DDA_1, the difference between V_{MEAS} and half of VDD can represent the voltage difference between V_{SP21} and V_{SP22} as shown in Fig. 2.

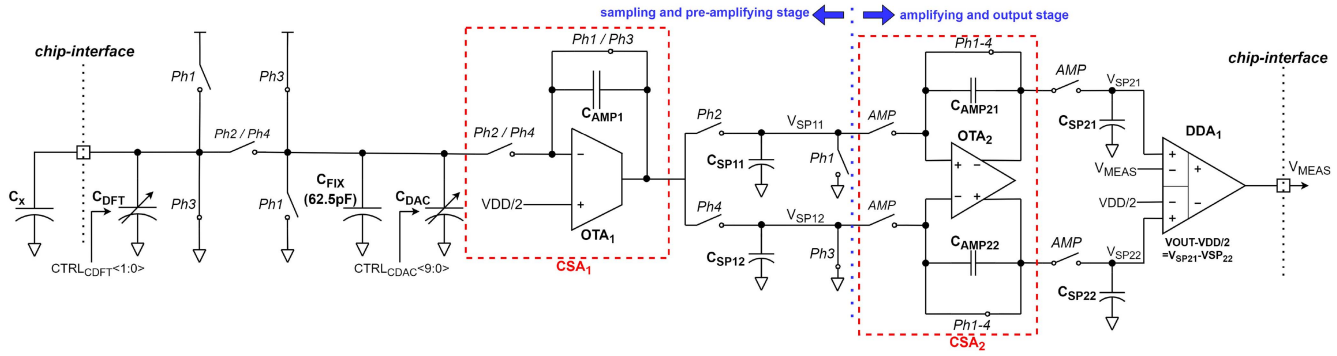

Fig. 2. Top-level schematic of the proposed readout circuit.

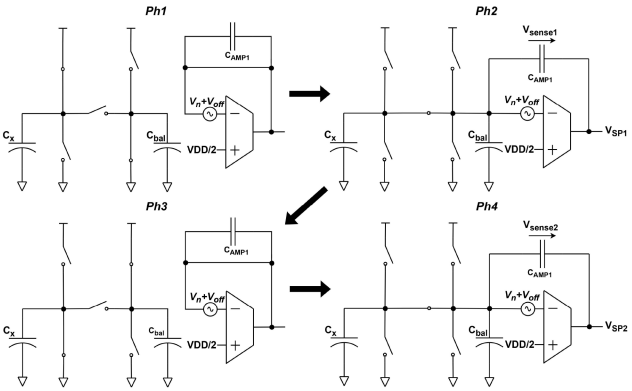

Fig. 3. Front-end circuit utilizing CDS.

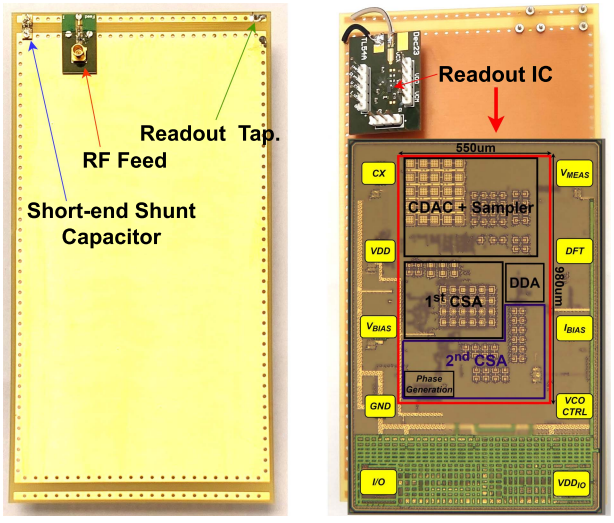

(a) (b)

Fig. 4. (a) Front side and (b) back side of the assembled sensor system along with the die micrograph of the implemented IC.

III. MEASUREMENT RESULTS

A. Characterization of the Readout IC

The readout IC was fabricated in a 90 nm RF SOI CMOS switch technology and its die micrograph is shown in Fig. 4(b). The core circuit consumes an area of 0.54 mm^2 and it is supplied by VDD of 1.8 V. The die has been bumped and flip-chip mounted on PCB for evaluation. Capacitor with a total capacitance value of 72 pF has been mounted on the evaluation board to emulate the offset capacitance of the sensor. The internal testing capacitor bank C_{DFT} was switched from 0 to 60 fF to characterize the sensitivity and noise floor of the readout IC, controlled by single-wire communication interface. The output signal of the readout IC, V_{MEAS}, was measured with Yokogawa DLM2024 oscilloscpoe and post-processed by a 2nd-order low-pass filter with a cutoff frequency of 500 Hz. The measured output waveform of the readout circuit is shown in Fig. 5(a). From the waveform, the readout IC shows a sensitivity of 2.51 mV/fF and a peak-to-peak noise of 42 mV, corresponding to a capacitance noise floor of 17 fF.

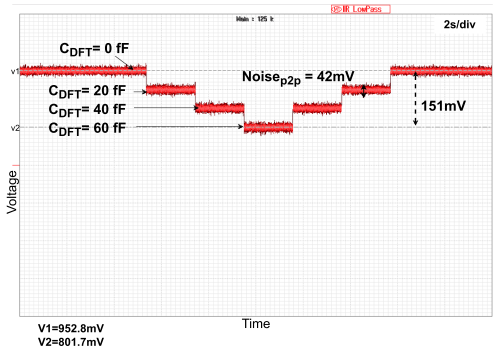

(a)

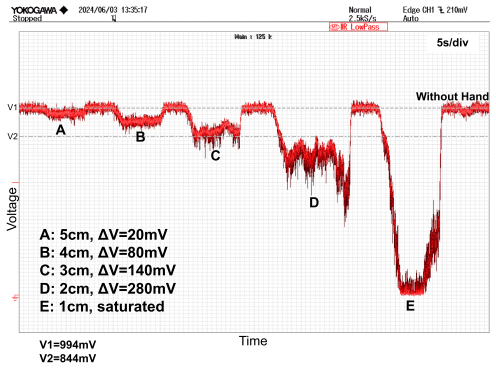

(b)

Fig. 5. Measured output signal (a) with C_{DFT} switched to various capacitance values and (b) with hand approaching to the sensor at different distances.

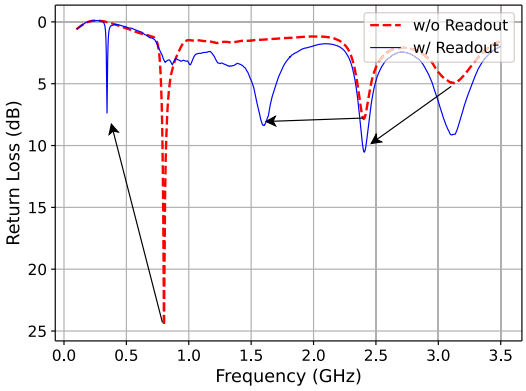

Fig. 6. Measured return loss of the IFA.

During the readout process, the readout IC consumes an average power of 365.4 μW.

B. Measurement With the Complete Sensor System

A prototype using an IFA as capacitive sensor with the readout IC attached to its backside has been assembled, and the photograph is shown in Fig. 4. Qualitative evaluation has been performed to verify the implemented sensor system. Human hand with dry skin was positioned at various distances from the prototype while the output signal of the readout IC was recorded simultaneously. The result is shown in Fig. 5(b). The output voltage returns to the original level immediately once the hand is removed, showing the repeatability of the proposed sensor system. For the distances below 1 cm, the readout circuit will be saturated by the increased sensing capacitance. The measured return loss of the IFA with and without the readout circuit is shown in Fig. 6. The presence of the readout circuit shifted the resonant frequencies towards lower frequencies due to the additional electrical length added to the radiating arm. Moreover, capacitive parasitics of the readout circuit can further increase the effective electrical length of the radiating arm [15]. The influence on RF performance can be mitigated with a more compact design and by connecting the readout IC to the IFA via an RF choke.

IV. CONCLUSION

In this letter, a proximity detection system using an IFA as the capacitive sensor with a dedicated readout IC is presented. In order to maintain the RF performance of the IFA, large offset capacitance has to be added in parallel to the sensing capacitor formed by the radiating arm of the IFA. The front-end circuit of the readout IC utilizes CDS procedure to reduce the negative effect induced by the offset capacitance. A novel sampling circuit is designed to apply the CDS scheme to the single-ended one-side-grounded IFA-integrated sensor. As a result, the readout IC shows a noise floor of 17 fF in the presence of a total offset capacitance of 72 pF. The assembled prototype demonstrates the feasibility of the IFA-integrated capacitive sensor with the implemented readout IC as a proximity detection system as well. To the best of the authors' knowledge, this letter is the first research paper, which demonstrates an IFA-integrated proximity capacitive sensor alongside with a dedicated readout IC.

REFERENCES

[1] Int. Comm. on Non-Ionizing Radiation Protection (ICNIRP), "Guidelines for limiting exposure to electromagnetic fields (100 kHz to 300 GHz)," *Health Phys.*, vol. 118, no. 5, pp. 483–524, 2020.

[2] C.-T. Chuang, T. Chang, P.-H. Jau, and F.-R. Chang, "Touchless positioning system using infrared LED sensors," in *Proc. IEEE Int. Conf. System Sci. Eng.*, 2014, pp. 261–266.

[3] X. Chen et al., "Development of a low-cost ultra-tiny line laser range sensor," in *Proc. IEEE/RSJ Int. Conf. Intell. Robots Syst.*, 2016, pp. 111–116.

[4] Z. Tong et al., "An ultrasonic proximity sensing skin for robot safety control by using piezoelectric micromachined ultrasonic transducers (PMUTs)," *IEEE Sensors J.*, vol. 22, no. 18, pp. 17351–17361, Sep. 2022.

[5] Y. S. Kim, S.-I. Cho, D. H. Shin, J. Lee, and K.-H. Baek, "Single chip dual plate capacitive proximity sensor with high noise immunity," *IEEE Sensors J.*, vol. 14, no. 2, pp. 309–310, Feb. 2014.

[6] SX9320 PerSe Connect, "High Performance 2-ch. SAR Sensor, Semtech, 2021, rev. 4. [Online]. Available: https://www.semtech.com/products/perse-smart-sensing/perse-connect/sx9320

[7] S. Myllymäki, A. Huttunen, V. K. Palukuru, H. Jantunen, M. Berg, and E. T. Salonen, "Feasibility study of antenna integrated capacitive sensor in operational mobile phone," *Prog. Electromagnetics Res. C*, vol. 23, pp. 219–231, 2011.

[8] A. Huttunen, M. Berg, S. Myllymäki, H. Jantunen, and E. T. Salonen, "Capacitive sensing of antenna loading with an R–C voltage divider in a tunable antenna," *IEEE Sensors J.*, vol. 13, no. 2, pp. 849–853, Feb. 2013.

[9] V. Solomko, O. Oezdamar, R. Weigel, and A. Hagelauer, "Penta-band inverted-F antenna tuned by high-voltage switchable RF capacitors," *IEEE Open J. Antennas Propag.*, vol. 2, pp. 375–384, 2021.

[10] O. Oezdamar, A. Hagelauer, R. Weigel, and V. Solomko, "Hardware toolkit for rapid prototyping of antenna tuning systems," in *Proc. IEEE Asia-Pacific Microw. Conf.*, 2019, pp. 509–511.

[11] C. Enz and G. Temes, "Circuit techniques for reducing the effects of op-amp imperfections: Autozeroing, correlated double sampling, and chopper stabilization," *Proc. IEEE*, vol. 84, no. 11, pp. 1584–1614, Nov. 1996.

[12] H. Ha, D. Sylvester, D. Blaauw, and J.-Y. Sim, "12.6 A 160nW 63.9fJ/conversion-step capacitance-to-digital converter for ultra-low-power wireless sensor nodes," in *Proc. IEEE Int. Solid-State Circuits Conf. Dig. Tech. Papers*, 2014, pp. 220–221.

[13] P. Yang, Z. Zhang, and N. Mei, "A 0.15mm^2 energy-efficient single-ended capacitance-to-digital converter," *IEEE Trans. Circuits Syst. II: Exp. Briefs*, vol. 69, no. 2, pp. 314–318, Feb. 2022.

[14] E. Sackinger and W. Guggenbuhl, "A versatile building block: The CMOS differential difference amplifier," *IEEE J. Solid-State Circuits*, vol. 22, no. 2, pp. 287–294, Apr. 1987.

[15] C. Rowell and R. Murch, "A capacitively loaded PIFA for compact mobile telephone handsets," *IEEE Trans. Antennas Propag.*, vol. 45, no. 5, pp. 837–842, May 1997.